Phase smearing and magnetic interaction in lead

P. M. Everett
Department of Physics and Astronomy, University of Kentucky, Lexington, Kentucky 50406

C. G. Grenier
Department of Physics and Astronomy, Louisiana State University, Baton Rouge, Louisiana 70803

(Received 26 September 1977)

Previous measurements of magnetic interaction on the de Haas–van Alphen effect in Pb were found to be in contradiction with the Shoenberg conjecture if a uniform magnetic induction was assumed to exist over the sample. A detailed numerical calculation of the de Haas–van Alphen effect has been developed that includes the phase smearing due to crystalline imperfections proposed by Shoenberg. It is found that reasonable, although substantial, amounts of phase smearing can account for these results. The g factor for the [110] γ orbit is treated as one of the fitting parameters, and a determination is made of it.

I. INTRODUCTION

The Shoenberg conjucture[1] (SC) proposes that the electron-electron magnetic interaction can be accounted for by replacing the applied field with the magnetic induction in the Lifshitz-Kosevich[2] (LK) noninteracting theory for the de Haas–van Alphen (dHvA) effect. We have previously reported the results of an investigation of the magnetic interaction effect in ellipsoidal samples of Pb,[3] referred to hereafter as I, which could not be accounted for by substituting the sample averaged magnetic induction into the LK theory. Since it is the induction on the scale of the electron's cyclotron orbit that is appropriate for the SC, one reason for this could be that the sample averaged induction differs from that averaged over a cyclotron orbit. The results of this investigation tend to support this possibility.

Shoenberg[4] has suggested that the presence of macroscopic crystalline imperfections can cause a smearing of the dHvA phase. This phase smearing is produced by slight shifts in the dHvA frequency over the volume of the sample. While such phase smearing does not reduce the local amplitude of the dHvA oscillations, as is the case with scattering, it does cause the various portions of the sample to be out of phase with one another. In this way the sample averaged oscillatory contribution to the magnetization can be substantially reduced from that averaged over a cyclotron orbit. Phase smearing then can cause a spatial inhomogenity in the magnetic induction. We show below that the results of I can be explained within the context of the SC with reasonable, although substantial, amounts of phase smearing.

II. CALCULATION

In I the period of the weak high-frequency α oscillation along ⟨110⟩ in Pb was measured as a function of the applied magnetic field. Along this crystallline direction there are only two other dHvA oscillations, called γ, which have frequencies somewhat less than one ninth that of the α oscillation and form a beat pattern of some 42.8 oscillations. An antinode of this beat pattern occurs in the vicinity of 50.7 kG, and at this field and a temperature of 1 K the combined γ oscillation is strong enough to cause a substantial modulation of the apparent α frequency. The ellipsoidal samples were cut so that ⟨110⟩ directions were along the longest and shortest of the ellipsoid axes. The samples were rotated *in situ*, and the primary results from I are the apparent frequency extremes along these two crystallographically equivalent directions with substantially different demagnetizing factors in each of the samples.

To compare with the experimental results, the dHvA effect must be solved for the application of the SC to the LK result. An exact analytical solution is not possible because of the self-consistency. We have developed a numerical method of calculating the observed signal that retains any desired number of dHvA harmonics and is limited only by the fineness of the grid over which the calculation is made and our understanding of the phenomena involved. The LK result modified by the SC for the ith dHvA oscillation is

$$M_i = M_{0i} \sum_{n=1}^{\infty} \frac{T}{B^{1/2} n^{1/2}} \frac{\exp[-nqm_i^*(T+X_i)/B]}{1-\exp(-2nqm_i^* T/B)} \times \cos\left(\frac{n\pi g_i m_i^*}{2}\right) \sin\left(\frac{2n\pi f_i}{B} + n\phi_i \pm \frac{\pi}{4}\right), \quad (1)$$

where T is the sample temperature, B is the magnetic induction appropriate to a cyclotron orbit, $q = 146\,927$ G/K, m_i^* is the electron's cyclotron's mass in units of the free-electron mass, X_i is the scattering Dingle temperature, f_i is the

dHvA frequency, ϕ_i is the phase constant, and g_i is the spin-splitting factor. The absolute amplitude M_{0i} depends only on the curvature of the Fermi surface and is generally not known with any accuracy. The total oscillatory magnetization M is a sum of terms of the form of Eq. (1), one for each dHvA oscillation present. If the magnetization is uniform over the sample, the proper expression for B is

$$B = H + 4\pi(1-\eta)M \ , \tag{2}$$

where H is the applied field and η is the demagnetizing coefficient for ellipsoidal samples that varies from 0 for the infinite rod to 1 for the infinite disk. However, if the magnetization is not uniform another approach must be developed. We suppose with Shoenberg[4] that the lattice distortion causes a distribution of the dHvA frequency and therefore of the phase over the volume of the sample and that the sample may be approximated as a collection of regions of different shapes and phases over each of which the dHvA phase is constant. The induction within such a region will depend on H, the shape of the region, the phase within the region, as well as on the regions surrounding it. If we assume that the effect of the surrounding regions is equivalent to a homogeneous medium of the volume averaged magnetization $\bar{M}$, the induction within the region is given by

$$B_{p,s} = H + 4\pi(1-\eta_s)M_{p,s} - 4\pi(\eta-\eta_s)\bar{M} \ , \tag{3}$$

where $M_{p,s}$ is the magnetization within the region and η_s is the local demagnetizing factor depending on the region's shape. The dHvA phases (p) and the shapes (s) of the regions are distributed over the sample volume. We suppose that the two distributions may be treated as statistically independent. If an average is first taken over the region shapes,

$$\bar{B}^s_{p,s} = H + 4\pi \bar{M}^s_{p,s} - 4\pi\overline{\eta_s M}^s_{p,s} - 4\pi(\eta-\bar{\eta}^s_s)\bar{M} \ . \tag{4}$$

This may also be written

$$B_r = H' + 4\pi(1-\eta')M_r \ , \tag{5}$$

$$H' = H - 4\pi(\eta-\eta'')\bar{M} \ , \tag{6}$$

where $B_r = \bar{B}^s_{p,s}$, $M_r = \bar{M}^s_{p,s}$, $\eta' = \overline{\eta_s M}^s_{p,s}/M_r$, and $\eta'' = \bar{\eta}^s_s$. If the regions have an effective spherical shape, which seems the most likely, we expect that $\eta' = \eta'' = \frac{1}{3}$. We will assume that $\eta' = \eta''$ and initially take it to be $\frac{1}{3}$. The magnetization within a region M_r is taken to be given by Eq. (1) with the field given by Eqs. (5) and (6). This magnetization is then phase averaged over the sample volume, as discussed below, to obtain $\bar{M}$. The "pseudofield" H' is a calculational convenience. It is uniform over the sample volume and amounts to the field to which each region is exposed.

In I detection was made with the field-modulation method, and the detected signal is proportional to $d\bar{M}/dt$, the phase averaged value of dM_r/dt. It is shown in Appendix A that the demodulated contribution at the lth modulation harmonic to dM_r/dt for the nth harmonic of the ith dHvA oscillation is given by

$$\frac{dM_{rni}}{dt} = -2l\omega M_{ni0} J_l(\lambda_{ni}) \sin(\Phi_{ni} + \tfrac{1}{2} l\pi) \ , \tag{7}$$

where the total dHvA amplitude has been written M_{ni0} and the total phase Φ_{ni}. The Bessel function argument depends on dM_r/dB_r and on its phase averaged value $d\bar{M}/dH'$. While it is possible to calculate $d\bar{M}/dH'$ exactly, much less computer time is used if we approximate it by $V(dM_r/dB_r)$, where V is a phase smearing coefficient described below. The results of the calculation, particularly the frequency modulation, are not measurably affected by this approximation, and we have used it in the interest of economy.[5] The calculation procedure is to select an appropriate range of values for B_r and calculate corresponding values for M_r and dM_r/dB_r from Eq. (1) and for H' from Eq. (5). Then, M_r is phase smeared as a function of H' to obtain $\bar{M}$, and H is calculated from Eq. (6). In the same steps dM_r/dt is calculated on the H' scale from Eq. (7) and phase smeared to obtain the detected signal on the H scale.

Shoenberg[4] has shown that for the cases in which the phase distributions over the sample for a high-frequency oscillation and a low-frequency oscillation are Lorentzian and are either statistically independent or completely correlated, the effect of the phase smearing is to multiply each frequency component in the dHvA spectrum by Dingle-like exponential factors. It has been shown previously,[6] referred to hereafter as II, that under the appropriate conditions, which are satisfied in Pb, the most likely case of partial correlation between the two phase distributions can be treated as fully correlated with appropriate interpretation of the phase smearing parameters and apparent high-frequency oscillation amplitude. Four phase smearing coefficients are appropriate for partial correlation, one each for the correlated and uncorrelated portions of the phases of the high- and low-frequency oscillations. Here we are applying the same phase smearing to both γ oscillations which seems reasonable since the cyclotron orbits are of almost the same size and shape. If u refers to the α oscillation, v to the combined γ oscillation, the subscript u to uncorrelated smearing, and the subscript c to correlated smearing, it is

shown in II that in the case of $u_c > v_c$, the effect of phase smearing is to reduce the α oscillation by $(u_u u_c)$. the nth harmonic of the γ oscillation by $(v_u v_c)^n$, and the mth sideband of the frequency modulated α oscillations by $u_u(v_u v_c)^{|m|} u_c^{\pm 1}$. The plus sign on the exponent of u_c occurs for positive correlation, positive sideband and negative correlation, negative sideband, and the minus sign occurs for the other two cases. Positive correlation refers to the case where the correlated portions of the phases of the two oscillations increase and decrease in the same portions of the crystal, while for negative correlation the one phase increases where the other decreases. The term positive sideband refers to the sum frequencies and negative sideband to the difference frequencies. Since u_u always occurs in the numerator with exponent 1, it can be absorbed directly into the local or unsmeared α amplitude, and since v_u and v_c always appear as a product they can be replaced by a single phase smearing coefficient V. Thus, in the phase smearing calculations each sideband is reduced by a factor $V^{|m|} u_c^{\pm 1}$. Phase smearing must be applied to both M_r and dM_r/dt. To accomplish this M_r and dM_r/dt were Fourier expanded on the H' scale. The frequency components were reduced by the appropriate phase smearing factors, and the functions were recalculated by integrating the reduced Fourier components. While the phase smearing occurs on the H' scale, the experimental filtering occurs on the H scale. To complete the determination of the calculated signal, $d\bar{M}/dt$ was Fourier expanded on the H scale and its frequency components reduced to correspond to the experimental filtering. The reduced components were integrated to give the calculated signal which was plotted against H^{-1}. This reproduced the chart recording and alternate zero crossings were used to determine the frequency modulation in the same manner as with the experimental data. The calculated signal shown in Fig. 1 corresponds to the experimental result shown in Fig. 4(b) of I. The calculated results then were treated very much in the same manner as the experimental results. Great care was exercised in I to remove any possible systematic bias in determining the frequency modulation. However, if any did remain it should have been treated equally in the determination of both the experimental and calculated results and not affect the conclusions of this investigation.

III. RESULTS

The effect of magnetic interaction on the α magnetization is to generate sidebands, and the result on the H' scale is a frequency modulated α oscillation. However, as has been pointed out by Shoenberg and Vuillemin[7] and Alles and Lowndes,[8] the frequency modulation introduces an amplitude

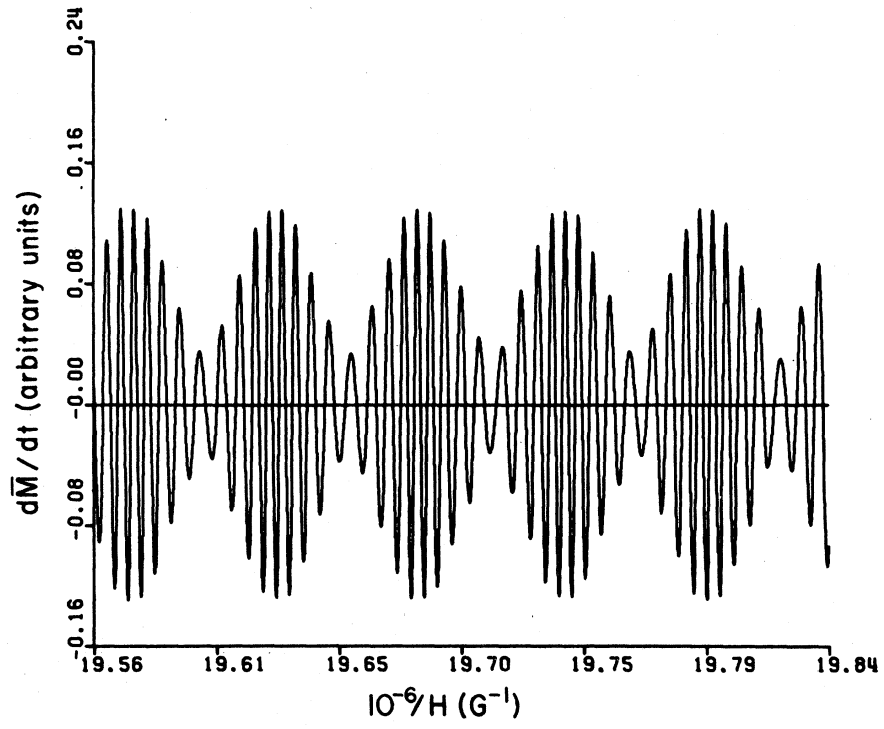

FIG. 1. Calculated α oscillation for the fit obtained in sample 3 with $g_\gamma = 6.25$ and second harmonic detection. The amplitude of the modulation field $h = 1.94$ G, the appropriate experimental filtering has been applied, $\eta = 0.056$, and $\eta' = \frac{1}{3}$. The other calculation parameters are given in Table II. This corresponds to the experimental result shown in Fig. 4 of I except that eddy current effects have not been included.

modulation into dM_γ/dt. This FM-AM effect alters the frequency modulation slightly through the amplitude modulation of $\bar{M}$ in Eq. (6). Phase smearing appreciably affects both the frequency and amplitude modulations. Plummer and Gordon[9] have shown that the effect of eddy currents is to produce an effective skin depth that oscillates with the γ frequency. The sample volume contributing to the detected signal then oscillates introducing an additional contribution to the amplitude modulation. However, since this occurs on the H scale, the frequency modulation is not affected. Hornfeldt, Ketterson, and Windmiller[10] have shown that an inhomogeneous applied field also affects the amplitude modulation on the H' scale. However, in I the applied field was sufficiently homogeneous that the effects on both the amplitude and frequency modulations were negligible. Thus, the frequency modulation is generated directly by magnetic interaction and is altered almost exclusively by phase smearing and to a much lesser degree by the FM-AM effect. On the other hand, while the amplitude modulation of the magnetization is generated partly by phase smearing, it is generated for the most part through the experimental artifacts such as the FM-AM effect and eddy currents, and the significant eddy current contribution can only be crudely estimated as discussed below. Thus the primary results of I are taken to be the frequency modulations of samples 2, 3, and 4 at two crystallographically equivalent $\langle 110 \rangle$ directions with different η.

In order to perform the calculation the values of the parameters in Eq. (1) must be known. The temperature was measured and the values for the dHvA frequencies and the phases were extracted from the data. The values for the cyclotron masses were taken from Phillips and Gold[11] and the orbit assignment from Anderson, Lee, and Stone.[12] Unfortunately, the total Dingle temperature, scattering plus phase smearing, were not measured. Thus the X_i in Eq. (1) were not known for a choice of the phase smearing parameters. The phase smearing equivalent temperatures evaluated here are large. Since these are good samples, the scattering contribution to the Dingle temperature must be fairly small. We find that the frequency modulation is not much affected as long as X_γ is not larger than 1 K. It is rather unlikely that the scattering Dingle temperatures are as large as this, and the X_i's in Eq. (1) were arbitrarily set to 0.2 K. The frequency modulation is determined by the amplitudes and phases of the sidebands. The leverage we have over the phases is through the LK harmonic content. The spin-splitting g factors have a much more pronounced effect on the LK harmonic content than do the X_i's, and the values selected for the g's do significantly affect the frequency modulation. In the calculation, we arbitrarily selected the same value for the g factors of both γ oscillations. Phillips and Gold[11] have proposed the value of $g_\alpha = 4.7$, but have not determined a value for g_γ. The above value for g_α was used in the calculation, but the α oscillation is sufficiently weak that the result is unaffected by this choice. The value of η' was initially set to $\frac{1}{3}$ and later varied to determine its effect. The unknown parameters that affect the calculation are the absolute amplitudes, g_γ, u_c, and V. The relative amplitudes were determined from the data, and the absolute amplitudes were represented by the single parameter $a_\gamma = 8\pi(M_{\gamma_1 10} f_{\gamma_1} + M_{\gamma_2 10} f_{\gamma_2})/H^2$ which is the net local or unsmeared a factor at the beat pattern antinode. Since the second LK harmonic will have a more pronounced effect than the higher harmonics, we initially considered three sets of values for g_γ: those for which $\cos(\pi g_\gamma m_\gamma^*)/\cos(\frac{1}{2}\pi g_\gamma m_\gamma^*) = 1, 0, -1$. As it turned out, the spin splitting zero for the second harmonic, the zero value for the above ratio, allowed us to fit the data quite well, while we were not as successful for the other two cases. Within the first modulus the four values of g_γ that result in $\cos(\pi g_\gamma^* m_\gamma^*) = 0$ are 0.89, 2.68, 4.46, and 6.25. The spin-splitting cosine factor for the third harmonic has the same magnitude as that of the fundamental but opposite sign for all four g_γ values. However, the spin-splitting cosine factor of the fourth harmonic has the opposite sign from the fundamental for the first and last g_γ values, while for the two middle values it has the same sign. The next distinction occurs for the eighth harmonic. As discussed below, we find that we can obtain a better all around fit with the data for $g_\gamma = 6.25$ than we can for $g_\gamma = 2.68$. We will present the results for $g_\gamma = 6.25$ and later discuss the effect of varying it.

Although the quality of the data for sample 4 of I was as good as it was for that of sample 3, the data for sample 3 was somewhat more abundant, and we will use the results of sample 3 to determine the best values for g_γ and η'. Values were selected for η', g_γ, u_c, and V and the calculation was performed over a range of a_γ values incremented by 0.05. The calculated signal $d\bar{M}/dt$ was plotted against H^{-1} to display the amplitude modulation. The frequency modulation determined from alternate zero crossings was also plotted against H^{-1}, and the maximum and minimum apparent frequencies were determined by sketching a smooth curve through these plots.[13] The maximum and minimum apparent frequences were plotted against a_γ and the curves corresponding to $\eta' = \frac{1}{3}$, $g_\gamma = 6.25$, and $u_c = V = 1$ (i.e., zero phase

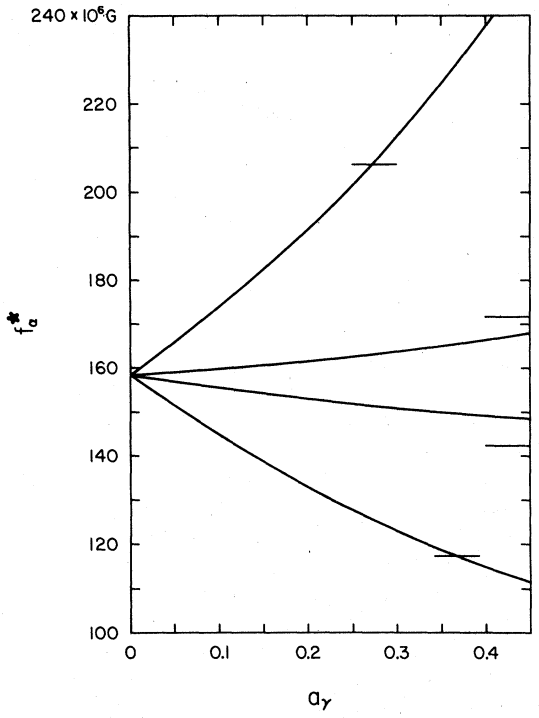

FIG. 2. Calculated frequency modulation for sample 3 with no phase smearing, $\eta' = \frac{1}{3}$, and $g_\gamma = 6.25$ vs the amplitude of the γ oscillation a_γ. The outer curves correspond to the small demagnetizing orientation $\eta = 0.056$ and the inner curve to the large demagnetizing orientation $\eta = 0.859$. The experimentally determined maximum and minimum apparent frequency values are shown as horizontal lines. The experimental values for $\eta = 0.859$ intersect the calculated curves at a_γ values that are greater than those plotted.

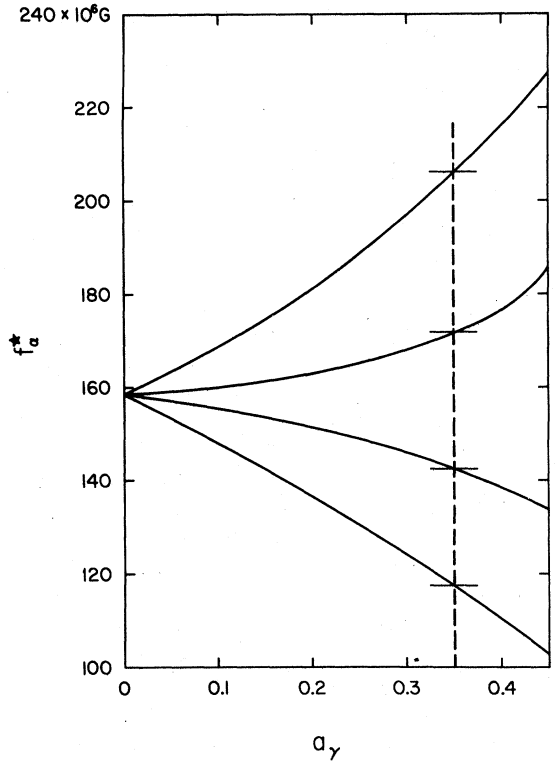

FIG. 3. Calculated frequency modulation for sample 3 that is the same as that shown in Fig. 2 except phase smearing has been included with $u_c = 0.88$ and $V = 0.60$. The intersections with all four of the experimental values (horizontal lines) are within 0.5×10^6 G of the calculated values at $a_\gamma = 0.35$.

smearing) are shown in Fig. 2. The outer curves correspond to the small demagnetizing factor in sample 3 and the inner curves to the large demagnetizing factor. The experimentally determined values are shown as horizontal lines. If the calculation reproduces the experiment, all four of these lines should intersect the curves at the same value of a_γ, and they clearly do not. The values of u_c and V were varied for both positive and negative correlation until a good fit was obtained. The curves for $u_c = 0.88$, $V = 0.60$, and negative correlation are shown in Fig. 3. The experimental values intersect the curves at $a_\gamma = 0.35$ within 0.5×10^6 G which is much less than the experimental uncertainty. The fit appears to be unique in that no other fit could be found for other choices of u_c and V and either positive or negative correlation.

The value of η' was set to 0.2, while the values of the other parameters were retained. The experimental frequency values fit to within 1×10^6 G, which is still within the experimental uncertainty, at $a_\gamma = 0.31$. The value of η' was set to 0.5, and the fit was within 2×10^6 G at $a_\gamma = 0.39$. These fits could most likely be improved with small variations of u_c and V. This variation of a_γ with η' is more or less what should be expected. As η' is increased the contribution of M_γ to B_r is decreased and the amplitude of the oscillation must be increased to compensate for it. It is also apparent that the fitted values for u_c and V are only weakly affected by the value for η' at least in the vicinity of $\frac{1}{3}$.

The value of g_γ was set to 7.14 for which the spin splitting factors are 1 for all harmonics. A search was made for values of u_c and V from 0.6 to 1 and for both positive and negative correlation. No fit to near the experimental uncertainty was found. Next g_γ was set to 3.57 where the spin splitting factors are -1 for the odd harmonics and $+1$ for the even harmonics. The best fit that could be obtained was to within 2×10^6 G for $u_c = V = 0.6$ and negative correlation. While this fit is not as good as that obtained with $g_\gamma = 6.25$, it cannot be rejected out of hand. The value of g_γ was set to 2.68, and a fit to within 0.5×10^6 G was obtained

TABLE I. Comparison of the experimentally determined γ line shape and α amplitude modulation with that calculated for the three fits obtained for Sample 3 of I. See Fig. 4 for definitions of A and ΔH^{-1}.

Calculation parameters				$\eta=0.859$			$\eta=0.056$		
g_γ	a_γ	u_c	V	$A+/A-$	$\Delta H_{inc}^{-1}/\Delta H_{dec}^{-1}$	m_a	$A+/A-$	$\Delta H_{inc}^{-1}/\Delta H_{dec}^{-1}$	m_a
2.68	0.35	0.88	0.66	0.98	0.77	0.28	0.99	0.53	0.50
3.57	0.30	0.60	0.60	0.95	0.57	0.50	0.99	0.39	0.78
6.25	0.35	0.88	0.60	0.98	0.85	0.22	0.97	0.61	0.58
Experimental values				0.96 ± 0.03	0.87 ± 0.04	0.55 ± 0.03	0.96 ± 0.03	0.61 ± 0.04	0.77 ± 0.04

for $u_c=0.88$ and $V=0.66$ at $a_\gamma=0.35$. The inverting of the fourth LK harmonic seems to alter V by about 10%, but leaves the other fitting parameters more or less unaffected. The values of g_γ and V also directly affect the line shape of the γ oscillation. While we cannot properly account for the eddy currents, it is clear that the effective skin depth oscillates as $-dM/dH$ and will be $\frac{1}{2}\pi$ out of phase with the signal detected at the second harmonic of the modulation frequency. The relative magnitudes and field positions of the extrema of the γ oscillation detected at the second harmonic will not be affected by the eddy currents. A comparison of these quantities taken from the calculated and experimental line shape should be meaningful and be an indication of the appropriateness of the choice of g_γ. The experimental zero line was obtained from the node of the γ beat pattern where magnetic interaction effects are negligible. The ratios of the positive to negative extrema of the γ oscillation for the two orientations of sample 3 are given in Table I together with the corresponding ratios of the calculated line shape for the values of g_γ for which fits were obtained. This information is not useful in that all the calculated ratios lie within the uncertainty of the experimental values. The ratios of the inverse field intervals of the increasing to decreasing portions of the γ signal are also given in Table I. The calculated γ line shape for the fit obtained with $g_\gamma=6.25$ is shown in Fig. 4 and the quantities given in Table I are indicated on it. Good agreement with experiment was obtained for $g_\gamma=6.25$, while the differences in the experimental and calculated values are well outside the experimental uncertainty for the other two values of g_γ. The amplitude modulations of the calculated signals for these three g_γ values are also compared to the experimental values in Table I. The values listed in Table I are defined in terms of the maximum and minimum detected α amplitudes over a γ oscillation by

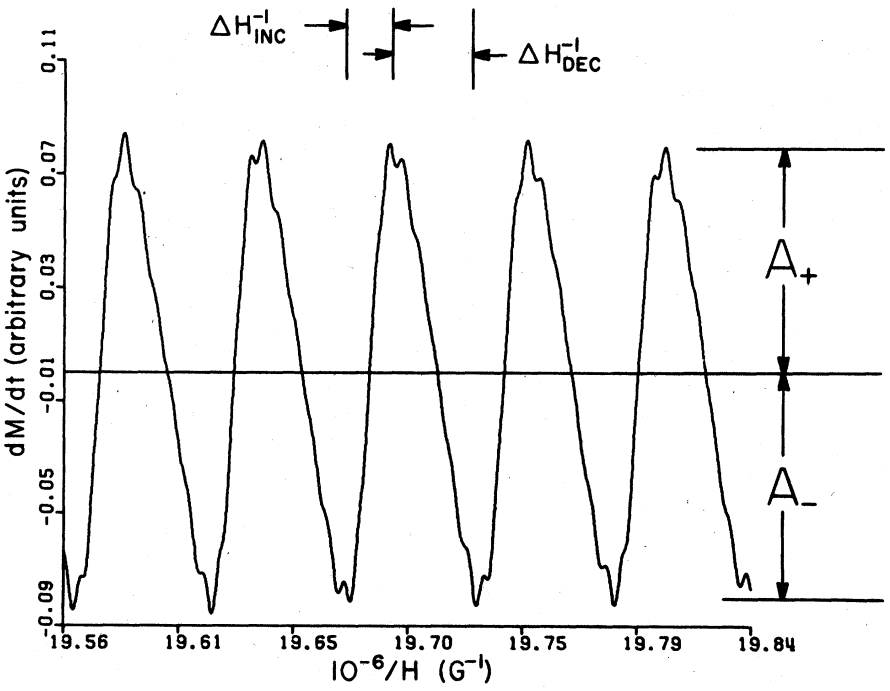

FIG. 4. Calculated γ oscillation for the fit obtained with $g_\gamma=6.25$ in sample 3. This differs from Fig. 1 in that $h=31$ G and no experimental filtering has been applied. The α oscillation is evident as it is in the data. The lineshape parameters given in Table I are indicated here.

$$m_a = (A_{max} - A_{min})/(A_{max} + A_{min}) \ .$$

Eddy currents have not been included in the calculation but do make a significant contribution to the amplitude modulation. The problem has been solved by Plummer and Gordon only for the infinite rod. Sample 3 for the small demagnetizing direction looks like an "edge-on" plate. If we assume that the rod solution is applicable for this orientation in sample 3 we find that m_a should be increased by about 0.15.[14] As seen in Table I, adding this to the value of $m_a = 0.58$ for $g_\gamma = 6.25$ accounts for nearly all of the amplitude modulation observed in sample 3 for $\eta = 0.056$. We are not in a position to make a similar comparison for $\eta = 0.859$, where the sample shape is very definitely not rodlike. Thus, it appears that $g_\gamma = 6.25$ gives very close to the observed harmonic content, and we conclude that g_γ is close to 6.25 or one of its corresponding values. The calculated α oscillation for the fit obtained with $g_\gamma = 6.25$ is shown in Fig. 1. The amplitude modulations were determined from plots of this type.

The frequency modulations of samples 2 and 4 of I were also fit for $\eta' = \frac{1}{3}$ and $g_\gamma = 2.68$ and 6.25. The results for the best frequency fits obtained for all three samples are shown in Table II with the experimental results.[15] The agreement with the experimental results for all three samples with $g_\gamma = 6.25$ and for samples 3 and 4 with $g_\gamma = 2.68$ is actually nearly 0.5×10^6 G. While the experimental uncertainty makes this sort of agreement not too meaningful, the ability to gain such agreement does point out the sensitivity of the calculation to the values of u_c and V. The best fits that could be obtained for sample 2 with $g_\gamma = 2.68$ and for sample 3 with $g_\gamma = 3.57$, while still within the experimental uncertainty were not nearly this good. The width of the spread of the α frequency over the sample volume caused by the correlated portion of the smearing, $\delta f_{\alpha c}$, is related to u_c by

$$u_c = \exp[\,(-2\pi(\delta f_{\alpha c})/H]\ ,$$

with corresponding expressions for the other three phase smearing parameters. The nth harmonic of a dHvA oscillation is multiplied by such factors raised to the nth power. It is convenient to define a Dingle-like Shoenberg, or phase-smearing, temperature by

$$S_{c\alpha} = -H(\ln u_c)/qm_c^* \ .$$

The correlated and uncorrelated Shoenberg temperatures add to the scattering contribution to give the total Dingle temperature. The correlated α and the total γ Shoenberg temperatures defined in this way are also listed in Table II.

The uncertainties in the fitting parameters can

TABLE II. Comparison of the experimental and calculated frequency modulation for the various fits obtained for samples 2, 3, and 4 of I. The dHvA frequencies are in units of 10^6 G, and the Shoenberg temperatures S are in K.

	Calculation parameters						Calculated results						Experimental results					
							Large demagnetizing orientation			Small demagnetizing orientation			Large demagnetizing orientation			Small demagnetizing orientation		
Sample	g_γ	a_γ	u_c	$S_{c\alpha}$	V	$S_{c\gamma}+S_{u\gamma}$	η	f^*_{max}	f^*_{min}	η	f^*_{max}	f^*_{min}	η	f^*_{max}	f^*_{min}	η	f^*_{max}	f^*_{min}
2	2.68	0.35	0.83	0.059	0.65	0.267	0.828	173	140	0.068	204	114	0.828	173±1	141±2	0.068	204±1	113±3
	6.25	0.34	0.85	0.051	0.60	0.317		173	141		205	113						
3	2.68	0.35	0.88	0.040	0.66	0.258	0.859	172	143	0.056	206	117	0.859	172±1	142±1	0.056	206±2	117±3
	3.57	0.30	0.60	0.161	0.60	0.317		171	141		204	118						
	6.25	0.35	0.88	0.040	0.60	0.317		172	142		207	118						
4	2.68	0.39	0.85	0.051	0.80	0.138	0.592	184	130	0.050	216	113	0.592	184±2	129±2	0.050	216±3	114±3
	6.25	0.38	0.88	0.040	0.66	0.258		184	130		215	113						

best be estimated by noting the effect of their variation on the frequency modulation. Variation of u_c and V by 0.02 and a_γ by 0.01 move the calculated frequency modulation over the experimental uncertainty. This places uncertainties on the Shoenberg temperatures of about 0.001 K on $S_{c\alpha}$ and 0.02 K on $(S_{c\gamma} + S_{u\gamma})$.

IV. DISCUSSION

The anomalous frequency modulation of I has been accounted for with reasonable amounts of phase smearing by including local demagnetization. We were not able to obtain a fit neglecting local demagnetization.[16] While the local-field approximation given by Eqs. (5) and (6) is certainly not exact, some degree of local demagnetization is necessary to account for the experimental results. As well, the γ harmonic content must be properly included. The calculation is sensitive enough to the fitting parameters that the uncertainties in these parameters are reasonable, and any error in them is due to the appropriateness of the model rather than to the fitting.

The amount of computer time required to perform this calculation precluded us from varying g_γ as we would have liked. It was fortunate that the value of $g_\gamma = 6.25$ reproduced the γ line shape so well. Considering the uncertainties in the experimental values any better agreement would be meaningless. However, by varying g_γ about 6.25 we could obtain an uncertainty for this fitting parameter. Hopefully, we will do this in the future when the appropriateness of the model is somewhat better established.

Samples 2 and 3 were cut from directly adjacent portions of the same boule while sample 4 was cut from an entirely different boule. We would expect samples 2 and 3 to have the same impurity and dislocation content. The dislocations and to a lesser degree the impurities will cause local lattice variations in a more or less random manner. Since the sizes of the α and γ cyclotron orbits differ substantially, this mechanism will contribute to both the correlated and uncorrelated parts of the phase smearing parameters and cause partially correlated phase smearing. The way in which the samples were prepared lent itself to an orientational smearing which would be primarily correlated. The samples were etched into ellipsoids, placed on a flat quartz plate, and annealed for three days at a temperature 7 °C under the melting point, and at this elevated temperature the edges may well have sagged. One ⟨110⟩ axis was perpendicular to the plate, and with this sagging it would have been tilted away from the normal near the perimeter of the sample introducing an angular dispersion. However, it is doubtful that the correlated smearing was produced in this way. Sample 4 had much more mechanical strength than samples 2 and 3 which had very nearly the same shape. However, u_c has the same value for samples 3 and 4 and a somewhat smaller value for sample 2. The difference in the values for u_c are within the combined uncertainties, and as far as can be determined all three samples have the same correlated smearing of the α oscillation. Since sample 4 was cut from different material it may well have had lesser impurity and/or dislocation contents than the other samples. In this case, the uncorrelated smearing of the γ oscillation would have been less which might well account for the larger value of V, and the scattering would also have been less which could account for the larger value of a_γ. This is also consistent with samples 2 and 3 having the same values for V and a_γ.

While it seems clear that there should be some degree of correlation between the phase smearings of the α and γ oscillations, it is not so obvious whether the smearings are positively or negatively correlated. Since the metal is compensated, positive correlation might be expected for an isotropic lattice distortion. However, negative correlation would not be unexpected for uniaxial strain. Dislocations, which we think are the primary cause of the lattice distortion, cause for the most part a uniaxial strain. Since the results are fit with negative correlation and not positive correlation, this view tends to be supported.

Phillips and Gold[11] have determined possible g values for the π, β, and δ orbits on the third zone hole surface in Pb by comparing their experimentally measured oscillation amplitudes with those predicted by the nonlocal pseudopotential calculation of Anderson, O'Sullivan, and Schirber.[17] One possible value for the δ orbit along ⟨111⟩ is 6.10 which is the closest to 6.25 for the possible g values of any of these three orbits. The closest possible values for the π and β along [110] are 9% and 6% below 6.25, respectively. Gold and Schmor[18] have determined possible values of g for the β orbit along [100] by a very precise method of comparing the amplitudes of the first three dHvA harmonics. Although there does not seem to be a direct correspondence between the possible values determined by the two methods, Gold and Schmor do obtain a possible value of 6.12 which is quite close to the value of 6.10 obtained by Phillips and Gold. However, Gold and Schmor are able to make an unambiguous determination of $g = 2.01 \pm 0.03$ when they compare their results to the pseudopotential calculation of Ref. 17. No evaluation has yet been made for either of the γ g factors or an

average of them. It is certainly not necessary nor expected that the g factor averaged over a cyclotron orbit be the same over the entire third zone hole sheet of the Fermi surface. However, the difference from 6.25 to 2.01 is fairly large and perhaps more than might be expected, and a value of $g_\gamma = 2.68$ might be closer to what one might expect. The distinction between $g_\gamma = 2.68$ and 6.25 is made entirely on the line shape of the γ oscillation and the amplitude modulation of the α oscillation. As seen in Table I the fits are most likely fortuitously good and the tendency is to put unwarranted confidence in them. The dHvA amplitudes are affected in so many ways in the presence of magnetic interaction that one can not be really sure that all the significant effects have been properly taken account, and any conclusions drawn from amplitude data must be somewhat suspect. While it is clear that g_γ is near a spin-splitting zero for the second harmonic, not too much confidence should be placed in our ability to distinguish between these possible values based on amplitude data and the effect of inverting the phase of the fourth harmonic.

ACKNOWLEDGMENTS

A substantial expression of gratitude is due to Cathy G. Elstrott for reducing the amplitude modulation data as well as some of the frequency data in I. Thanks are especially due to Professor D. Shoenberg for sending the results of his work prior to publication and for a very informative visit. We also gratefully acknowledge a conversation with Professor W. L. Gordon. This work was supported in part by the Research Corporation.

APPENDIX A

In the local-field approximation used here we assume that the electron carries out its orbit in an ellipsoidal region throughout which the magnetic induction B_r is constant in magnitude and phase. The shape and orientation of the region corresponds to an effective demagnetizing factor η'. The magnetization within such a region is $M_r(B_r)$ and the volume averaged magnetization is $\bar{M}(H')$ with the fields given by Eq. (5) and (6). If a time oscillating field of angular frequency ω and amplitude h is superposed on the quasistatic applied field H, M_r and $\bar{M}$ are then functions of

$$B_r^* = H'^* + 4\pi(1-\eta')M_r(B_r^*) ,$$

$$H'^* = H + h\sin\omega t - 4\pi(\eta-\eta')\bar{M}(H'^*) ,$$

respectively. Since h is much smaller than H in these experiments $M_r(B_r^*)$ and $\bar{M}(H'^*)$ can be expanded about B_r and H', respectively,

$$M_r(B_r^*) \simeq M_r(B_r) + \left.\frac{dM_r}{dB_r^*}\right|_{B_r}(B_r^* - B_r) = M_r(B_r) + \left.\frac{dM_r}{dB_r^*}\right|_{B_r}\{4\pi(1-\eta')[M_r(B_r^*) - M_r(B_r)]$$
$$- 4\pi(\eta-\eta')[\bar{M}(H'^*) - \bar{M}(H')] + h\sin\omega t\} ,$$

$$\bar{M}(H'^*) \simeq \bar{M}(H') + \left.\frac{d\bar{M}}{dH'^*}\right|_{H'}(H'^* - H') = \bar{M}(H') + \left.\frac{d\bar{M}}{dH'^*}\right|_{H'}\{-4\pi(\eta-\eta')[\bar{M}(H'^*) - \bar{M}(H')] + h\sin\omega t\} .$$

These equations may be solved to yield

$$M_r(B_r^*) - M_r(B_r) \simeq \frac{a_r}{4\pi}\,\frac{1-\bar{a}/(1+\bar{a})}{1-a_r'}\,h\sin\omega t ,$$

$$\bar{M}(H'^*) - \bar{M}(H') \simeq (\bar{a}/4\pi)(1+\bar{a}')^{-1}\,h\sin\omega t ,$$

where

$$a_r = 4\pi\left.\frac{dM_r}{dB_r^*}\right|_{B_r} , \quad \bar{a} = 4\pi\left.\frac{d\bar{M}}{dH'^*}\right|_{H'} ,$$

$$a_r' = (1-\eta')a_r , \quad \bar{a}' = (\eta-\eta')\bar{a} .$$

The time-dependent local field may be written

$$B_r^* = B_r + \Gamma h\sin\omega t ,$$

with

$$\Gamma \simeq 1 + a_r'\,\frac{1-\bar{a}'/(1+\bar{a}')}{(1-a_r')} - \frac{\bar{a}'}{(1+\bar{a}')} .$$

The nth harmonic of the ith oscillation may be written

$$M_{ni} \simeq M_{0ni}\sin\left(\frac{2\pi n f_i}{B_r + \Gamma h\sin\omega t} + n\phi_i \pm \tfrac{1}{4}\pi\right) ,$$

where the field and temperature dependence have been absorbed into M_{0ni}. Since $\Gamma h \ll B_r$, the argument may be expanded;

$$M_{ni} \simeq M_{0ni} \sin[\,\Phi_{ni} - \lambda_{ni} \sin\omega t\,] \ ,$$

$$\Phi_{ni} = 2\pi n f_i / B_r + n\phi_i \pm \tfrac{1}{4}\pi \ ,$$

$$\lambda_{ni} = (2\pi n f_i / B_r^2)\Gamma h \ .$$

The standard Bessel-function expansion may be differentiated to yield

$$\frac{dM_{rni}}{dt} \simeq -2l\omega M_{0ni} \sum_{l=1}^{\infty} J_l(\lambda_{ni}) \times \sin(\Phi_{ni} + \tfrac{1}{2}l\pi) \sin(l\omega t + \tfrac{1}{2}l\pi) \ .$$

The total detected signal is obtained by summing over all dHvA harmonics of all oscillations present.

---

[1]D. Shoenberg, Philos. Trans. R. Soc. Lond. A 255, 85 (1962). The SC proposes that this many body interaction can be taken into account by using the magnetic induction as the proper field in the LK noninteracting theory.

[2]I. M. Lifshitz and A. M. Kosevich, Zh. Eksp. Teor. Fiz. 29, 730 (1955) [Sov. Phys.-JETP 2, 636 (1956)].

[3]P. M. Everett and C. G. Grenier, Phys. Rev. B 15, 3826 (1977).

[4]D. Shoenberg, J. Low. Temp. Phys. 25, 751 (1976).

[5]In the local-field modulation technique described in Appendix A, the local modulation amplitude is given by Γh, where $\Gamma(dM_r/dB_r, d\bar{M}/dH')$ is approximated by $\Gamma(dM_r/dB_r, VdM_r/dB_r)$. This substitution, which is equivalent to a slight variation of the modulation field amplitude, h, is found to have a negligible effect on the zero crossings of the calculated signal and, therefore, on the determination of the calculated frequency modulation. Thus, the substitution of VdM_r/dB_r for $d\bar{M}/dH'$, which is not generally justifiable, is appropriate for this computing step.

[6]C. G. Grenier and P. M. Everett, Phys. Lett. 63A, 371 (1977).

[7]D. Shoenberg and J. J. Vuillemin, *Proceedings of the Tenth International Conference on Low Temperature Physics, Moscow*, 1966, edited by M. P. Malkov (Viniti, Moscow, 1975).

[8]H. Alles and D. H. Lowndes, Phys. B 8, 5462 (1973).

[9]R. D. Plummer and W. L. Gordon, Phys. Lett. 20, 612 (1966).

[10]S. Hornfeldt, J. B. Ketterson, and L. R. Windmiller, J. Phys. E 6, 265 (1973).

[11]R. A. Phillips and A. V. Gold, Phys. Rev. 178, 932 (1969).

[12]J. R. Anderson, J. V. M. Lee, and D. R. Stone, Phys. Rev. B 11, 1308 (1975).

[13]Since the field interval over a γ oscillation contains not quite nine α oscillations, each oscillation in the apparant α frequency contained no more than nine calculated values. The maximum and minimum apparent frequency values were determined by sketching a smooth curve through these points over several γ oscillations, and there was some uncertainty in the maximum and minimum values due to this discreteness. However, this uncertainty was not considered in this discussion, because it was less than the experimental uncertainty which in addition contained the contribution from the detection system stability and general experimental noise.

[14]The eddy current induced amplitude modulation was incorrectly stated in I as being 15% of that caused by the FM-AM effect. Rather it adds 0.15 to the m_a produced by the FM-AM effect.

[15]The value listed in I for $f^*_{\min}$ at the $\eta = 0.068$ orientation in sample 2 was 118×10^6 G instead of the correct value of 113×10^6 G. The error occurred in transcribing the average frequency value. In Table I of I the value of $f_\alpha/f^*_{\max}$ for $\eta = 0.068$ should be 1.399 ± 0.014 and the values of the calculated parameters should be $a_\gamma = 0.272 \pm 0.017$, $b = 1.21 \pm 0.06$, $b_{\min} = 1.17 \pm 0.04$, $b_{\max} = 1.30 \pm 0.05$, and weighted average $= 1.23 \pm 0.05$. The error is not significant and does not affect the analysis or conclusions of I.

[16]It was assumed that $B = H + 4\pi(1-\eta)M$. The calculation was made in a similar fashion to the above: M_r, dM_r/dt, and H were calculated over a selected range of B; the calculated signal was Fourier expanded, phase smeared, filtered, and integrated to obtain the detected signal.

[17]J. B. Anderson, W. J. O'Sullivan, and J. E. Schirber, Phys. Rev. B 5, 4683 (1972).

[18]A. V. Gold and P. W. Schmor, Can. J. Phys. 54, 2445 (1976).